water

MDPI

Article

The Crustal Vertical Deformation Driven by Terrestrial Water Load from 2010 to 2014 in Shaanxi–Gansu–Ningxia Region Based on GRACE and GNSS

Wanqiu Li [1], Jie Dong [2], Wei Wang [2], Yulong Zhong [3], Chuanyin Zhang [2], Hanjiang Wen [2], Huanling Liu [2], Qiuying Guo [1,*] and Guobiao Yao [1]

[1] School of Surveying and Geo-Informatics, Shandong Jianzhu University, Jinan 250101, China; 24106@sdjzu.edu.cn (W.L.); yao7837005@sdjzu.edu.cn (G.Y.)
[2] Chinese Academy of Surveying & Mapping, Beijing 100830, China; dongjie@casm.ac.cn (J.D.); wangwei@casm.ac.cn (W.W.); zhangchy@casm.ac.cn (C.Z.); wenhj@casm.ac.cn (H.W.); liuhl@casm.ac.cn (H.L.)
[3] School of Geography and Information Engineering, China University of Geosciences (Wuhan), Wuhan 430078, China; zhongyl@cug.edu.cn
* Correspondence: qyguo@sdjzu.edu.cn

Abstract: The terrestrial water resources in Shaanxi–Gansu–Ningxia (SGN) region are relatively scarce, and its climate change is unstable. Research on the deformation driven by terrestrial water load is of great significance to the dynamic maintenance of reference station networks. In this paper, data derived from Gravity Recovery and Climate Experiment (GRACE) and Global Navigation Satellite System (GNSS) from 2010 to 2014 were combined to monitor the spatiotemporal characteristics of surface vertical deformation caused by terrestrial water load change. The single scale factor was calculated by comparing CPC, WGHM, and GLDAS hydrological model to restore filtering leakage signal. The singular spectrum analysis (SSA) method was used to extract the principal component of temporal vertical deformation, and its spatial distribution was analyzed. At the same time, in order to study the relationship between the terrestrial water load deformation from GRACE and that from GNSS, the first-order term correction, the Atmosphere and Ocean De-aliasing Level-1B product (GAC) correction, and the first-order load LOVE number correction for GRACE were adopted in this paper. In addition, a quantitative comparative analysis of both the monitoring results was carried out. The results show that the time-variable characteristics of surface vertical deformation characterized by the filtered three hydrological models were consistent with those of GRACE. The correlation coefficient and Nash–Sutcliffe efficiency coefficient (NSE) values were the highest in the GLDAS model and the GRACE model, respectively; the former index is 0.93, while the latter is 0.85. The crustal vertical deformation from terrestrial water load showed a declining rate from 2010 to 2014. Its spatial change rate showed an obvious ladder distribution, with the surface subsidence rate gradually decreasing from south to north. In addition, weighted root mean square (WRMS) contribution rate of the crustal vertical deformation resulting from GRACE with GAC correction between the different GNSS stations ranged from 18.52% to 54.82%. The correlation coefficient between them was close to 0.70. After deducting the mass load impact of GRACE only, the WRMS contribution rate of the corresponding stations decreased from −8.42% to 21.18%. The correlation coefficient between them reduced noticeably. Adding GAC back can increase the comparability with GRACE and GNSS in terms of monitoring the crustal vertical deformation. The annual amplitude and phase of surface vertical deformation resulting from GRACE with GAC correction were close to those of GNSS. The research results can help to explore the motion mechanism between water migration and surface deformation, which is of benefit in the protection of the water ecological environment in the region.

Keywords: GRACE; GNSS; crustal vertical deformation; GAC correction; SSA

check for updates

Citation: Li, W.; Dong, J.; Wang, W.; Zhong, Y.; Zhang, C.; Wen, H.; Liu, H.; Guo, Q.; Yao, G. The Crustal Vertical Deformation Driven by Terrestrial Water Load from 2010 to 2014 in Shaanxi–Gansu–Ningxia Region Based on GRACE and GNSS. *Water* **2022**, *14*, 964. https://doi.org/10.3390/w14060964

Academic Editor: Fausto Grassa

Received: 29 December 2021
Accepted: 14 March 2022
Published: 18 March 2022

1. Introduction

SGN region is an important economic zone for the development of the western region, and its environmental problems are characterized by wind erosion and desertification, soil erosion, and air pollution. It is one of the regions with the most serious ecological environment damage and soil erosion in China. Studying the changes of terrestrial water storage and its load deformation in the SGN region can be conducive to the improvement of the water resources environment and regional sustainable development; furthermore, it is of great significance for the dynamic maintenance of regional high-precision reference framework. GRACE's time-variable gravity field has made important progress in monitoring regional water load deformation, considering northern China [1,2], central Saudi Arabia [3], and the Degris Islands [4] as examples. A large number of research results reveal the influence of groundwater reduction in different depth aquifers on ground deformation, which has attracted great attention among scholars at home and abroad. In addition, GRACE can effectively monitor glacial isostatic adjustment, solid earth load deformation caused by climate change, such as ground rebound caused by melting of the South Greenland ice sheet [5], the annual surface change caused by heavy precipitation in Yunnan [6], and the elastic deformation of the Australian continent caused by LaNiña event and the water cycle [7].

However, most studies used the displacement data from GNSS to verify the reliability of GRACE monitoring results, mainly comparing the annual variation characteristics of the two results. Through comparative analysis, it was found that terrestrial water load deformation monitored by GRACE is mainly reflected in the vertical direction. As early as 2004, Davis found that the surface vertical deformation from water load change in the Amazon Basin was in good agreement with the annual change in GNSS radial displacement [8]. However, this consistency is poor in regions with small changes in water quality. Van Dam found that the main reason is that the processing model for GNSS data is inaccurate, resulting in false periodic signals [9]. After improving the processing model for GNSS data and method, Tregoning found that the correlation between the results and GRACE was significantly improved [10]. In addition to the water load migration, the physical factors affecting the vertical displacement of GNSS also include the surface temperature change, which can cause temperature change inside the surface cement pier of the GNSS antenna installed on the GNSS station. At the same time, the temperature change in the bedrock of the GNSS station is caused by the heat conduction mode, thus causing the vertical displacement change in the GNSS station [11,12].

In fact, the temperature effect is not included in the surface load deformation monitored by GRACE, and its spatial resolution is still insufficient to reflect the local high-frequency signals in the fine water storage load deformation, thus increasing the difference with GNSS monitoring [13–15]. However, with the optimization of data processing methods, the difference between the two is narrowing [16]. Godah [17] investigated the usefulness of national Continuously Operating Reference Station (CORS) networks, which provide GNSS data, for the determination of those temporal mass variations and for improving GRACE/GRACE-FO solutions. Wang analyzed the annual surface vertical displacement monitored by GRACE and the vertical time series from 29 continuous GNSS stations in northern China, and the results showed that both of the annual variation signals of vertical displacement had strong correlation characteristics [1]. Zhang used the time series of 35 GNSS stations to estimate the annual vertical deformation of the surface in Nepal, southern Himalaya, and compared GNSS with GRACE monitoring results [18]. Wang adopted the scale factor method to achieve the surface vertical load deformation in southern Greenland using GRACE, which was in good agreement with the observation time series from GNSS [5]. It was found that the elevation time series from GNSS contains the annual vertical surface deformation caused by changes in terrestrial water storage. Using GRACE to analyze the influence of vertical deformation from terrestrial water load on GNSS elevation time series has become a research hotspot in recent years. In addition, some scholars have studied the quantitative relationship between the surface horizontal deformation from GNSS and the corresponding results of GRACE. After investigating nearly 89% of GPS stations, Ray [19] indicated that a positive correlation can be determined between seasonal deformations of the Earth's surface in the northern area obtained from GPS and the corresponding ones from GRACE data.

In order to improve the comparability and consistency between GRACE monitoring results and GNSS in the SGN region, in this paper, first-order correction, first-order load LOVE number correction, GAC correction, and leakage error correction were added on the basis of GRACE spherical harmonic coefficient analysis results. In this paper, the SSA method was used to extract the vertical displacement characteristics from GRACE and GNSS. Compared with the direct least squares method of function fitting, the SSA method has the advantages of accurate signal extraction and can avoid the influence of sequence noise. The spatiotemporal distribution of results derived from GRACE was analyzed; furthermore, the results from both GRACE and GNSS were quantitatively compared, and the annual variation characteristics were also analyzed.

2. Data and Method

2.1. GRACE Data and Postprocessing

The GSM data from the GRACE gravity satellite were used in this paper, as derived from the Center for Space Research (CSR, the University of Texas at Austin). A level-2 (RL06) monthly gravity field model GSM was regularized by the SH coefficient, which deducts the effects of solid tides, ocean tides, solid polar tides, nontidal atmospheres, and oceanic influences, as well as gravity disturbances caused by other entities, such as the sun and the moon. The RL06 version of the GSM time series incorporates the same process of surface mass redistribution as the RL05 product.

We used GRACE RL06 data to invert the crustal vertical deformation, according to Equation (1). We used RL06 data, with a degree/order of 60. We did not truncate the degree/order 96 to degree/order 60 but directly employed the value of 60 [20,21]. As the GRACE earth gravity field model contains high-order term noise, in order to reduce the influence of high-order noise, many scholars [22,23] cut the order/degree of the spherical harmonic coefficient to 60. At the same time, the spatial resolution of the GRACE gravity satellite is about 330 km, and the corresponding order/degree is 60. The noise of the high-degree and high-order coefficients was processed by fan filtering with a smooth radius of 300 km [24,25]. The correlation error was corrected via P_3M_{15} decorrelation filtering. Here, the embedding dimension was 5, and the fitting order was 3. The coefficients of degree 1 were replaced by Sweason's results [26]. In addition, we modified the expressions of GRACE C_{20} values by replacing the C_{20} values from the CSR/GFZ/JPL-RL06 GSM files with the corresponding values from TN11. The TN11 values of SLR-derived C_{20} are not interchangeable with the TN07 or TN05 values, due to differences in background models and the absence of background rates in the former. For any month without data, the coefficients were derived by averaging values from two adjacent months.

2.2. GNSS Data

We adopted geodetic height data from 8 CORS stations, resulting from continuous GNSS observations in the SGN region from 2010 to 2014. The data processing was mainly carried out via GAMIT/GLOBK software. Using each station's daily GNSS data, single-day region relaxation solutions for station and satellite orbit were obtained. Based on the GAMIT-derived baseline solutions, the International GNSS Service core stations with good quality and evenly distributed were selected as fixed reference stations, which were adopted as constraints used in the GLOBK adjustment; then, the GLOBK was employed in joint adjustment to gain the time series of station coordinate changes under the ITRF2014 framework [27,28]. Solid tides, tidal ocean signals, and tidal atmospheric signals were removed, using the IERS 2010 protocol. SSA algorithm, combined with 3RMS criterion, was used for gross error detection and elimination, as well as interpolation compensation for missing data. The location of GNSS stations in the SGNR region is shown in Figure 1. In addition, the main parameters used in the GAMIT calculation are given in Table 1.

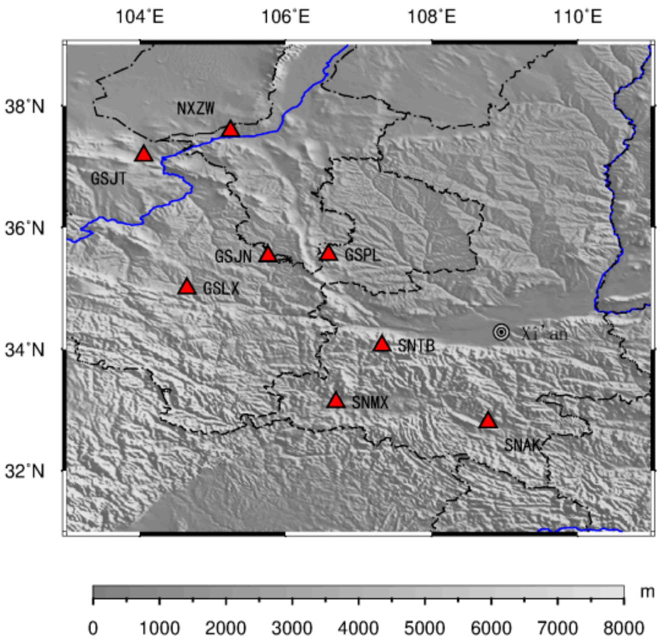

Figure 1. Location of GNSS stations in SGNR.

Table 1. The main parameters used in the GAMIT calculation.

Parameter	Processing Mode
Ionosphere delay model	LC_AUTCLN
Tropospheric model	Saastamoinen + GPT2w + estimation
Ambiguity resolution	LAMBDA method
Framework of prior coordinates	ITRF2014
Sampling interval data	15 s
Satellite cut-off elevation angle (°)	10
Solid tide model	IERS2010
Ocean tide model	FES2004(otl_FES2004.grid)
Inertial framework	J2000
Atmospheric mapping function	VMF1
Solar radiation pressure model	ECOMC model
PCO/PCV	IGS14 atx

2.3. Method

Farrell [29] states that if the spherical harmonic expansion of the surface load value is known, the radial displacement of the Earth caused by this load can be calculated via Equation (1). The smoothing function in Equation (1) is used to reduce high order noise existing in the time-variable gravity field model from GRACE [30]. Based on the elastic load theory, the vertical displacement of the surface detected by GRACE is calculated. The formula is as follows:

$$dr(\theta,\lambda) = \frac{3}{\rho_e}\sum_{n=0}^{\mathrm{Nmax}}\sum_{m=0}^{n}\frac{h'_n}{2n+1}\cdot P_{n,m}(\cos\theta)\cdot W_n\cdot W_m\cdot(\Delta C_{nm}\cdot\cos(m\lambda)+\Delta S_{nm}\cdot\sin(m\lambda)) \quad (1)$$

where $dr\ (\theta,\ \lambda)$ is the surface vertical deformation; θ and λ are the colatitude and longitude of the calculation point, respectively; $(\Delta C_{nm}, \Delta S_{nm})$ is the change in normalized SHCs with degree n and order m; $\overline{P}_{nm}(\cdot)$ is the fully normalized associated Legendre function with degree n and order m; $\rho_e = 5.5\times10^3\ \mathrm{kg/m^3}$ is the average density of solid earth; W_n and W_m are the degree-dependent and order-dependent smoothing functions, respectively [30].

The load Love numbers with PREM were obtained from the public data released by Hansheng Wang [31].

Tapley [32] indicated that it is reasonable to control the truncation of the model order below 90 order. Chen further revealed that the data above 60 order will introduce large errors [33]. Therefore, the spherical harmonic coefficient of the gravity model is usually truncated to 60 × 60 order, and its half-wavelength resolution can reach 333 km [34]. In this paper, the order and degree of the gravity field model were truncated to 60, that is, the maximum order/degree in Equation (1) was set to 60. In order to minimize the influence of leakage error on the surface vertical load deformation derived from GRACE in the SGN region, the scale factor method was selected to reduce the filtering effect. Specifically, first, the hydrological model was expanded to gravity spherical harmonics and filtered by the same process with GRACE. Then, the regional surface vertical load deformation was calculated to obtain the time series after spatial averaging. At the same time, the unfiltered gravity coefficients were used to calculate the inversion results. The corresponding scale factors can be calculated based on two time series—before filtering and after filtering. In order to ensure that GRACE monitoring results and GNSS data belong to the Center of Figure (CF) framework, the first-order correction on GRACE data has been completed, but the first-order load Love number conversion is still needed. In addition, the monthly average of GNSS elevation sequences is needed to unify the time resolution.

3. Result and Analysis

3.1. Leakage Error Correction with Single Scale Factor

In order to reduce the GRACE filtering loss, in this paper, a single scale-factor method was used to correct the leakage error. Three hydrological models—CPC, WGHM, and GLDAS—were used for spherical harmonic expansion, and the same filtering treatment as GRACE was used to estimate the surface vertical deformation caused by water load changes in the SGN region, the results of which were quantitatively compared with GRACE filtering results, which are shown in Figure 2. In order to quantitatively evaluate the correlation between the results from the hydrological model and GRACE in terms of phase and amplitude, the correlation coefficient and NSE index were adopted for quantitative calculation in this paper. Thus, the model closest to the time series of GRACE filtering results was selected to calculate the scale factor.

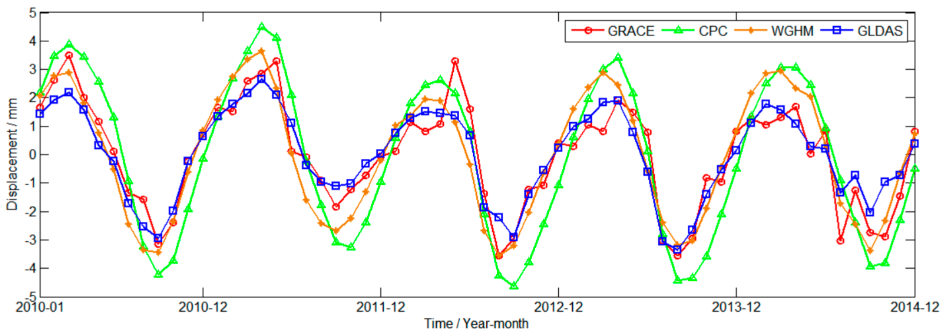

Figure 2. The crustal vertical deformation in SGN region driven by terrestrial water load represented by GRACE and three hydrological models from 2010 to 2014.

It can be seen from Figure 2 and Table 2 that the correlation coefficient between the vertical deformation from surface load represented by GLDAS and GRACE filtering results was 0.93, while the NSE reached 0.85. Compared with CPC and WGHM, the filtering results from GLDAS were closest to those from GRACE. This shows that soil water storage change within 0~2 m of surface depth in SGN was the main factor causing the spatiotemporal change in terrestrial water storage. Moreover, it indicates that the change in groundwater storage in SGN accounted for a relatively small proportion. Therefore, the scale factor k = 1.21 was calculated in the SGN region based on the two time series of the GLDAS model before and after filtering, to restore the leakage signal of GRACE. Then, we adopted the corrected results of GRACE to analyze its spatiotemporal distribution in the SGN region and compared them with those from GNSS.

Table 2. Correlation coefficients between surface vertical deformation of water load in three filtered hydrological models and GRACE in SGN from 2010 to 2014.

Three Hydrological Models	CPC	WGHM	GLDAS
Correlation coefficient/NSE	0.91/0.50	0.89/0.72	0.93/0.85

3.2. Spatiotemporal Analysis of Vertical Deformation from Terrestrial Water Load

In order to better analyze the spatial characteristics of the rate of surface vertical deformation caused by the change in terrestrial water load in the SGN region from 2010 to 2014, linear fitting for the monthly spatial grid of monitoring results was carried out to obtain the vertical deformation rate every year driven by terrestrial water load, from 2010 to 2014, as shown in Figure 3.

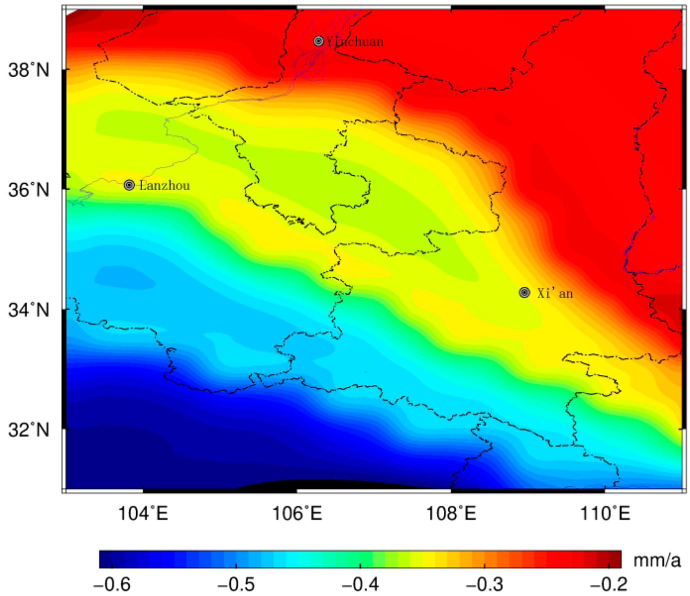

Figure 3. Linear rate every year for vertical deformation from terrestrial water load in SGN from 2010 to 2014.

As can be seen from Figure 3, from 2010 to 2014, changes in terrestrial water load in the study region caused a trend of surface subsidence year by year. This trend showed an obvious ladder distribution in spatial distribution, and the surface decline rate gradually decreased from south to north. The surface decline rates in the west and southwest of the study region were the most obvious, and the linear rate of surface vertical deformation was −0.6 mm/a. The surface decline degrees in the north and northeast were weak, and the linear rate was −0.2 mm/a.

In order to further analyze the time-variable characteristics of the vertical deformation of the overall terrestrial water load in the study region, the SSA method was adopted to decompose the time series and the overall variation sequence of the vertical deformation derived from the terrestrial water load. Then, the total time series with a yellow curve was decomposed into trend term, seasonal term, and residual term, as shown in Figure 4, with the black curve, red curve, and green curve, respectively.

It can be seen from Figure 4 that the vertical deformation derived from terrestrial water load in the SGN region was mainly seasonal. The analysis of trend items revealed that changes in terrestrial water load from 2010 to 2014 caused a trend of ground subsidence year by year. From the analysis of seasonal items, it can be found that the change in terrestrial water load in the SGN region caused the surface to produce upward vertical displacement from May to June each year. The maximum vertical displacement of ground uplift was 2.7 mm, and the maximum vertical displacement of ground subsidence was close to 3 mm from September to October each year. The time-variable characteristics of this seasonal vertical deformation were obvious, which may be related to seasonal precipitation. After extracting the trend and seasonal terms, the residuals had no obvious changing trend, which is probably due to human factors.

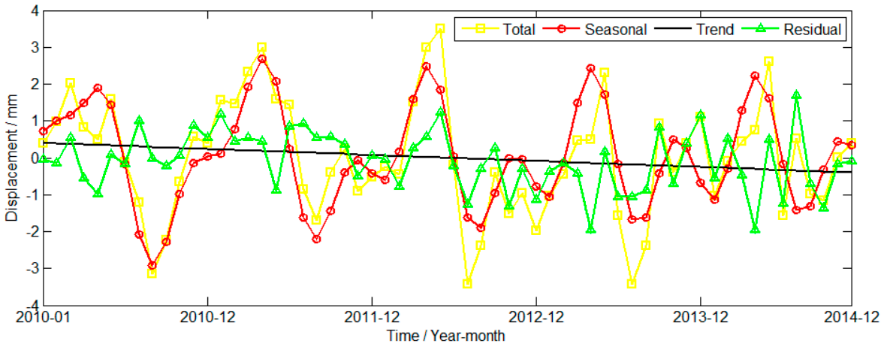

Figure 4. Vertical deformation series and decomposition signals of terrestrial water load in SGN from 2010 to 2014.

In order to analyze monthly and season spatial variation characteristics, in this paper, the spatial distributions of results from GRACE were plotted for a total of 20 months from February, May, August, November in 2010 to the same period in 2014, which are shown in Figure 5.

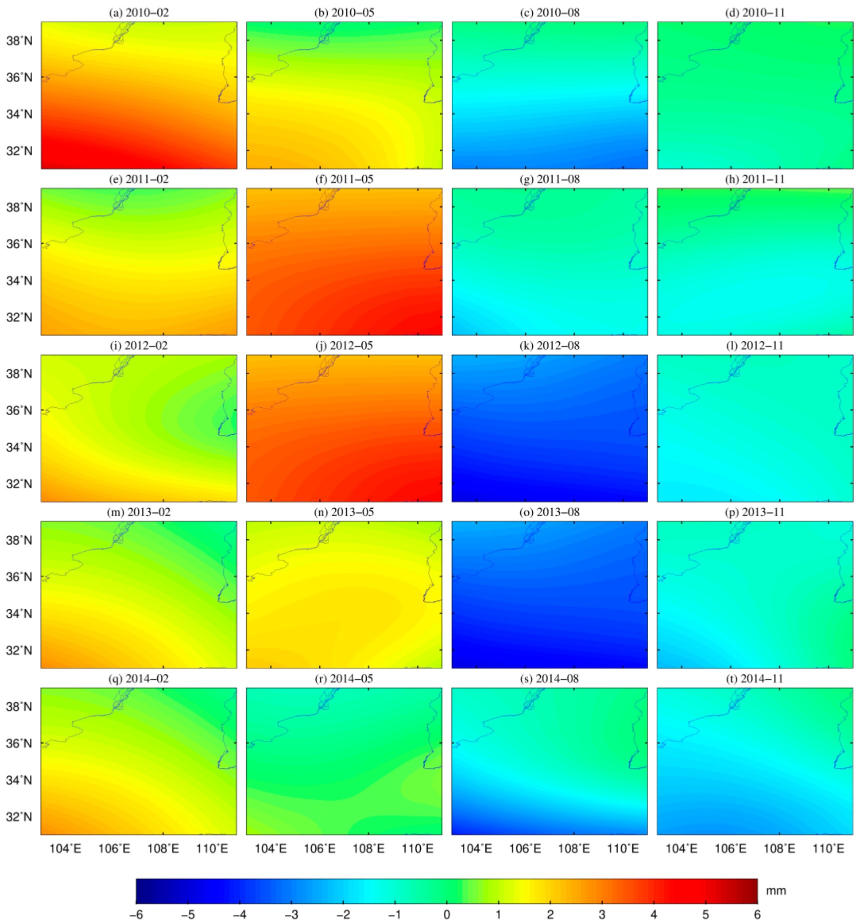

Figure 5. The monthly and seasonal vertical deformation maps driven by changes in terrestrial water load.

From Figure 5, it can be seen that the monthly vertical deformation of terrestrial water load in the SGN region had relatively obvious spatial heterogeneity. Signal intensity generally decreased from south to north. Seasonal variation in the signal spatial distribution in the study area was obvious. In winter and spring each year, the terrestrial water load decreased, resulting in an upward vertical deformation of the surface. By contrast, in summer and autumn each year, the terrestrial water load increased, resulting in downward vertical deformation of the surface. Considering the studied time periods, in the spring of 2011 and 2012, the surface of the study area had an obvious upward rebound, while in the summer of 2013 and 2014, terrestrial water load changes led to significant surface subsidence.

3.3. The Comparison of the Vertical Deformation from GRACE and GNSS

In order to quantitatively compare the consistency between the time series of GNSS elevation direction and the vertical displacement monitored by GRACE, in this paper, the reduction ratio of weighted root mean square (*WRMS*) was analyzed before and after removing GRACE signals from the GNSS sequence. The numerical results indicate the contribution of vertical deformation caused by surface quality load changes monitored by GRACE to GNSS elevation displacement. The calculation formula can be expressed as

$$WRMS_{\text{reduction}} = \frac{WRMS_{\text{GNSS}} - WRMS_{\text{GNSS}-\text{GRACE}}}{WRMS_{\text{GNSS}}} \quad (2)$$

Since the impact of nontidal atmosphere and high-frequency ocean signals has been deducted when solving GSM products, while GNSS coordinate sequences contain such signals, in order to make the comparison of background models consistent either the impact of GAC load should be added back to GSM or the GAC should be deducted from GNSS observations. In this paper, in order to facilitate the calculation, we chose to add GAC directly on the basis of GRACE GSM results [35,36], which means applying GAC correction to GRACE results to enhance the comparability of the two results. The vertical displacement sequence from GRACE before and after GAC correction was compared with the time sequence of CORS station elevation direction, as shown in Figure 6. Here, the red curve represents the time sequence of CORS station geodetic height. The blue curve indicates that only the leakage error was corrected on the basis of GRACE GSM data processing. The green curve indicates that the leakage error and GAC correction were carried out on the basis of GRACE GSM data processing. The relevant statistical results are shown in Table 3.

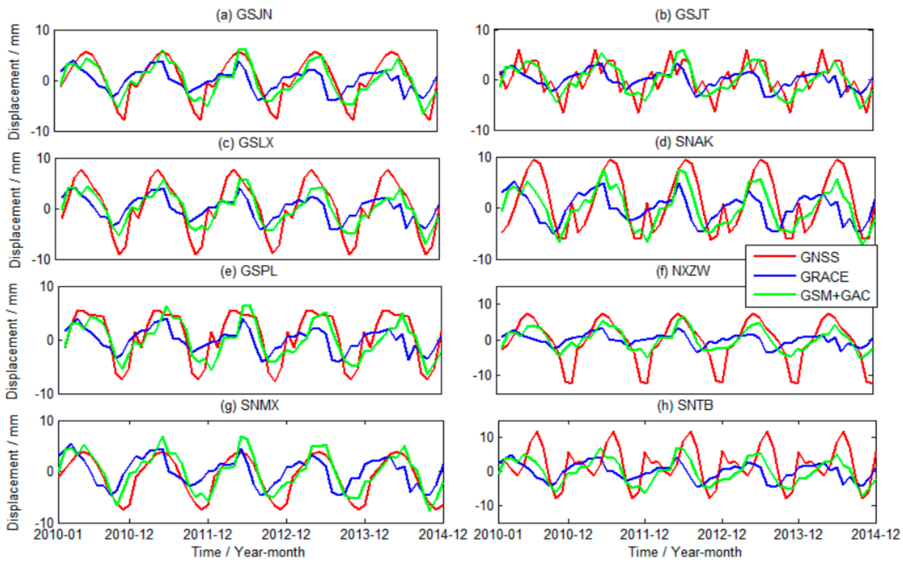

Figure 6. The crustal vertical displacement comparison with 8 CORS data and GRACE before and after GAC correction in SGN from 2010 to 2014.

Table 3. Correlation coefficient and contribution rate between vertical time series from GNSS and load vertical deformation derived from GRACE in SGN from 2010 to 2014.

Different Method	**GAC Correction**		**Without GAC Correction**	
Station Name	**Correlation Coefficient**	**WRMS Contribution Rate/%**	**Correlation Coefficient**	**WRMS Contribution Rate/%**
GSJN	0.89	52.79	0.55	16.53
GSJT	0.63	18.75	0.33	3.65
GSLX	0.88	45.59	0.65	21.18
GSPL	0.83	43.97	0.62	20.20
NXZW	0.78	31.48	0.22	2.37
SNAK	0.79	37.92	0.09	−8.42
SNMX	0.89	54.82	0.53	13.45
SNTB	0.58	18.52	0.10	−5.72

It can be seen from Figure 6 and Table 3 that the variation trends of the three time series on the overall time scale are well consistent. Most of the correlation coefficients between surface vertical displacement from GRACE with GAC correction and GNSS elevation time series were about 0.7. After the influence of GRACE and GAC load was deducted, the WRMS value of the GNSS elevation direction sequence decreased, and the contribution rate of GRACE to GNSS was within the range of 1.29~58.97%. When GAC correction was not considered, the WRMS value of the same station was also reduced after only deducting the GRACE mass load term, and the contribution rate was reduced to −5.72~21.18%. Therefore, this shows that the vertical displacement results based on GRACE are reliable. Additionally, this result reveals that the sensitivity of elevation displacement at different stations to regional terrestrial water load sources is different, based on the different contribution rates of surface vertical deformation caused by terrestrial water load derived from GRACE to GNSS elevation time series.

In order to compare the relationship between GRACE monitoring results and GNSS vertical displacement time series more clearly, GRACE results were deducted from GNSS vertical displacement sequence to obtain residual time series; then, GAC values were added to the GRACE results to obtain another residual sequence; both sequences are expressed with the red and green curves in Figure 7, respectively.

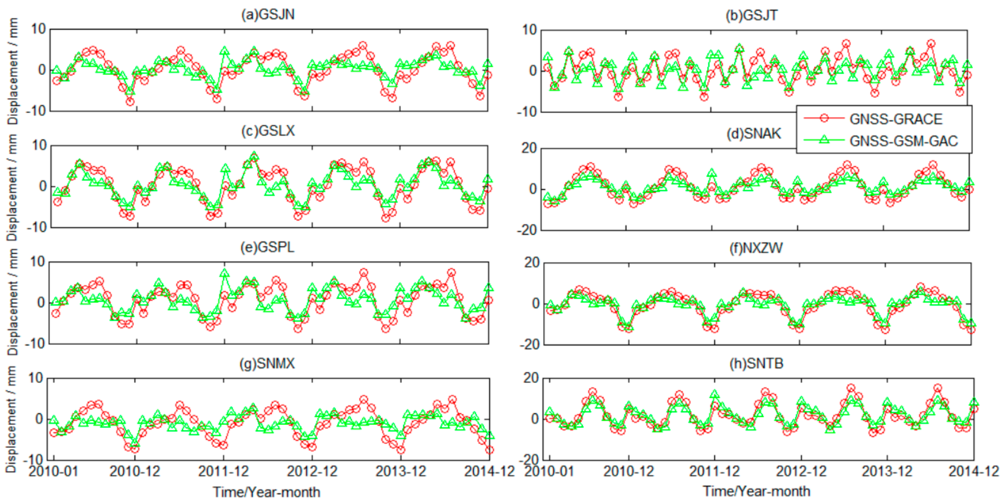

Figure 7. Residual sequences obtained by subtracting GRACE results before and after GAC correction from GNSS vertical displacement sequence.

From Figure 7, it can be found that the residual sequence obtained by deducting GRACE results from the vertical displacement time series of GNSS still had obvious amplitude changes. In addition to the GSJT station, the periodic characteristics of residual sequences from the other stations were very obvious. On this basis, after deducting the GAC results, the amplitude of each station residual sequence had different degrees of reduction. However, the periodic signal characteristics were still noticeable. This shows that the surface vertical displacement from GNSS in the SGN region still had periodic signals when deducting the terrestrial water load deformation and atmospheric ocean load deformation derived from GRACE and GAC; however, the reasons behind this result needs further study [37].

The amplitude of semiannual signals in GNSS elevation time series is relatively small, and the influencing factors are complex [15]. Therefore, in this paper, the focus was on the annual signal, for which a comparative analysis was carried out of the vertical displacement of the annual changes resulting from GNSS and GRACE. The SSA algorithm was adopted to extract the annual signal of both the vertical displacement time series [38,39], which are all shown in Figure 8. The red curve represents the elevation sequence from the CORS station, and the blue curve represents the vertical displacement derived from GRACE with GAC correction.

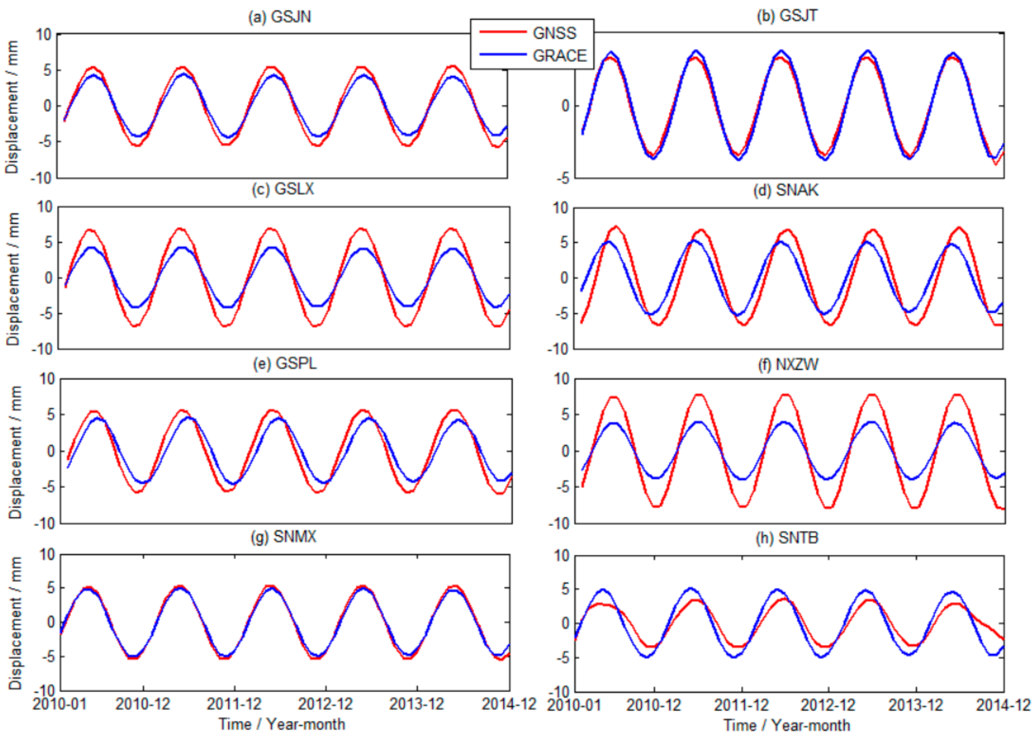

Figure 8. Comparison of GRACE and GAC total mass term time series with vertical time series from 8 CORS in SGN.

It can be seen from Figure 8 that the annual vertical displacement derived from GRACE with GAC correction fluctuated within the range of ±5~±20 mm. Its annual amplitude also changed over time. The annual change characteristic of vertical deformation from GRACE was consistent with that from GNSS on the whole. According to the annual signal extracted by SSA, the annual amplitude and phase of GRACE results and GNSS vertical displacement sequence were obtained by fitting the sine and cosine functions. The unit of fitted phase is rad; the relative statistical results are shown in Table 4.

It can be found from Figure 8 and Table 3 that the GRACE monitoring results with GAC correction were consistent with the overall variation trend of geodetic height time series from GNSS. In addition to SNTB CORS stations, the annual amplitude of vertical displacement from GRACE was smaller than that of GNSS at the same stations. According to the above analysis, on the basis of GRACE GSM results, adding GAC back increased the comparability with GNSS elevation time series to ensure that the two results were affected by the same load. The annual change in the GRACE results was consistent with the annual change in the CORS elevation time series. The results indicate that there was a 1~32 day delay between the annual vertical displacement of terrestrial water load from GRACE and the vertical time series from GNSS. It was also found that the amplitude of annual variation in GNSS elevation time series was not stable but changed with time. In line with the research idea of most scholars, in this paper, the constant amplitude was used for fitting, which inevitably increases the uncertainty of its annual amplitude calculation and will be further explored in subsequent studies [5,39].

Table 4. Statistical values of the vertical deformation from GNSS and the sum of GRACE and GAC in SGN from 2010 to 2014.

Station	GRACE		GNSS	
Statistic	Annual Amplitude/mm	Annual Phase/rad	Annual Amplitude/mm	Annual Phase/rad
GSJN	4.30 ± 0.06	-1.01 ± 0.03	5.61 ± 0.04	-0.90 ± 0.01
GSJT	3.60 ± 0.04	-1.08 ± 0.02	3.47 ± 0.06	-0.99 ± 0.03
GSLX	4.80 ± 0.05	-0.81 ± 0.02	7.03 ± 0.04	-0.70 ± 0.01
GSPL	4.99 ± 0.05	-1.10 ± 0.03	5.78 ± 0.06	-0.71 ± 0.01
NXZW	5.00 ± 0.04	-1.26 ± 0.01	8.00 ± 0.05	-1.25 ± 0.02
SNAK	5.12 ± 0.10	-0.99 ± 0.04	6.94 ± 0.09	-1.54 ± 0.03
SNMX	5.15 ± 0.03	-0.90 ± 0.03	5.46 ± 0.03	-0.87 ± 0.02
SNTB	4.62 ± 0.08	-1.02 ± 0.04	3.30 ± 0.17	-1.20 ± 0.10

4. Discussion

The gravity field changes monitored by GRACE are caused by the load effect of change in terrestrial water storage and also include other environmental changes and geodynamic effects, such as atmospheric ocean load, earthquakes, volcanoes, and geotectonic movements. These effects need to be deducted from observational data, especially GNSS observations. This is also an important factor affecting the difference between GRACE monitoring results and GNSS. At the same time, the thermal expansion effect causes the vertical displacement of the GNSS station. Jiang Weiping [40] found that the annual temperature of GNSS stations in the middle and high latitudes changed significantly, resulting in a maximum vertical displacement amplitude of 1.8 mm, while the average amplitude of low latitude stations was only 0.16 mm. It was found that the influence of thermal expansion deformation had obvious annual and semiannual periodic characteristics, and the average annual amplitudes of low-, medium-, and high-latitude stations were 0.12 mm, 0.60 mm, and 0.60 mm, respectively [40]. This effect was ignored in this paper, which is one of the important factors causing the difference in annual amplitude between the two monitoring results. With the continuous improvement of satellite gravity observation accuracy, it is necessary to increase the correction of thermal expansion effect when combining GRACE and GNSS to analyze the vertical deformation driven by terrestrial water load in the region, especially when analyzing the annual change. In addition, in this paper, a single scale-factor method was used to correct the leakage error caused by GRACE filtering [41,42]. The annual amplitude of some stations, such as SNTB results, was greater than that of GNSS, which may be due to the problem of over-recovering the leakage signal. In the next study, more appropriate methods on leakage error correction can be considered to gradually improve the consistency between GRACE and GNSS monitoring results. The residual vertical displacement from GNSS in the SGN region still had periodic signals when deducting the sum of deformation caused by terrestrial water load and GAC load from the vertical deformation sequence of GNSS stations; however, the underlying reasons of this result need further study [43].

5. Conclusions

In this paper, GRACE RL06 data were used to reveal the spatiotemporal changes in surface vertical deformation caused by terrestrial water load in the SGN region from 2010 to

2014. Three different hydrological models were used to quantitatively evaluate the correlation coefficient with GRACE monitoring results, and the scale factor was further calculated. At the same time, the GRACE monitoring results were compared with the GNSS elevation time series. In order to enhance the consistency between the two monitoring results, in this paper, the first-order correction, the first-order load Love number correction, the leakage error correction, and the GAC correction were used for GRACE results. The principal components of GRACE and GNSS were extracted by SSA and analyzed quantitatively. The results are as follows:

(1) The comparison results of three hydrological models showed that the correlation coefficient and NSE index of GLDAS model filtering results and GRACE filtering time series were closest to 1, indicating that the scale factor based on the results before and after filtering for GLDAS could effectively restore the GRACE leakage signal, and the scale factor $k = 1.21$ was calculated.
(2) The surface vertical deformation caused by terrestrial water load in the SGN region from GRACE showed obvious stepladder spatial distribution, and the deformation variables gradually decreased from south to north. The linear rate of surface vertical deformation in the southwest was -0.6 mm/a, while the linear rate in the north and northeast was less, with -0.2 mm/a.
(3) Compared with GNSS, the correlation coefficient and contribution rate of GRACE and GNSS changed significantly before and after GAC correction was applied to GRACE. This indicated that GAC correction is helpful to enhance the consistency between GRACE and GNSS. In addition, both of the annual variation trends were also relatively consistent, but the total mass amplitudes of GRACE and GAC were smaller than those of GNSS. The research results can help to explore the motion mechanism between water migration and surface deformation, which is of benefit in the protection of water's ecological environment in the region.

Author Contributions: Conceptualization, Q.G. and J.D.; methodology, W.L.; software, C.Z.; validation, W.L., W.W. and C.Z.; formal analysis, Y.Z.; investigation, H.L.; resources, C.Z., W.W.; data curation, C.Z.; writing—original draft preparation, W.L.; writing—review and editing, Q.G.; visualization, H.L.; supervision, Q.G.; project administration, H.W.; funding acquisition, G.Y. All authors have read and agreed to the published version of the manuscript.

Funding: This research was supported by the National Natural Science Foundation of China with Project No. 42171435; the Key Laboratory of Surveying and Mapping Science and Geospatial Information Technology of Ministry of Natural Resources, No. 2020-1-4; Doctoral Research Fund of Shandong Jianzhu University, No. X20086Z0101.

Institutional Review Board Statement: Not applicable.

Informed Consent Statement: Not applicable.

Data Availability Statement: Not applicable.

Acknowledgments: The authors would like to acknowledge the CSR for providing GRACE RL06 level-2 data. We are also grateful to the institutions and individuals providing CORS station data, and we thank the reviewers who provided their valuable comments for the revising of the paper.

Conflicts of Interest: The authors declare no conflict of interest.

References

1. Wang, L.; Chen, C.; Du, J.; Wang, T. Detecting seasonal and long-term vertical displacement in the North China Plain using GRACE and GPS. *Hydrol. Earth Syst. Sci.* **2017**, *21*, 2905–2922. [CrossRef]
2. Liu, R.; Zou, R.; Li, J.; Zhang, C.; Zhao, B.; Zhang, Y. Vertical Displacements Driven by Groundwater Storage Changes in the North China Plain Detected by GPS Observations. *Remote Sens.* **2018**, *10*, 259. [CrossRef]
3. Othman, A.; Abotalib, A.Z. Land subsidence triggered by groundwater withdrawal under hyper-arid conditions: Case study from Central Saudi Arabia. *Environ. Earth Sci.* **2019**, *78*, 243. [CrossRef]
4. Rateb, A.; Kuo, C.-Y. Quantifying Vertical Deformation in the Tigris-Euphrates Basin Due to the Groundwater Abstraction: Insights from GRACE and Sentinel-1 Satellites. *Water* **2019**, *11*, 1658. [CrossRef]

5. Wang, S.-Y.; Chen, J.L.; Wilson, C.R.; Li, J.; Hu, X. Reconciling GRACE and GPS estimates of long-term load deformation in southern Greenland. *Geophys. J. Int.* **2017**, *212*, 1302–1313. [CrossRef]
6. Zhan, W.; Li, F.; Hao, W.; Yan, J. Regional characteristics and influencing factors of seasonal vertical crustal motions in Yunnan, China. *Geophys. J. Int.* **2017**, *210*, 1295–1304. [CrossRef]
7. Han, S.C. Elastic deformation of the Australian continent induced by seasonal water cycles and the 2010-2011 LaNiña determined using GPS and GRACE. *Geophys. Res. Lett.* **2017**, *44*, 2763–2772. [CrossRef]
8. Sheng, C.Z.; Gan, W.J.; Liang, S.M.; Chen, W.T.; Xiao, G.R. Identification and elimination of non-tectonic crustal deformation caused by land water from GPS time series in the western Yunnan province based on GRACE observation. *Chin. J. Geophys.* **2014**, *57*, 42–52. (In Chinese)
9. Dam, T.V.; Wahr, J.; LavallÃ©e, D. A comparison of annual vertical crustal displacements from GPS and Gravity Recovery and Climate Experiment (GRACE) over Europe. *J. Geophys. Res. Solid Earth* **2007**, *112*, 1426–1435.
10. Tregoning, P.; Watson, C.; Ranmillien, G.; McQueen, H.; Zhang, J. Detecting hydrologic deformation using GRACE and GPS. *Geophys. Res. Lett.* **2009**, *36*, L1540. [CrossRef]
11. Yan, H.M.; Chen, W.; Zhu, Y.Z.; Zhang, W.M.; Zhong, M.; Liu, G.Y. Thermal effects on vertical displacement of GPS stations in China. *Chin. J. Geophys.* **2010**, *53*, 825–832. (In Chinese) [CrossRef]
12. Weijie, T.; Xueqing, X.; Danan, D.; Junping, C.; Bin, W. Thermoelastic seasonal deformation in Chinese Mainland. *Acta Geod. Et Cartogr. Sin.* **2017**, *46*, 1080–1087.
13. Lulu, J.; Hansheng, W.; Longwei, X. Measuring terrestrial water storage change using GRACE, GPS and absolute gravity data in Scandinavia. *Acta Geod. Et Cartogr. Sin.* **2017**, *46*, 170–178.
14. Renli, L.; Jiancheng, L.; Weiping, J.; Zhao, L. Comparing vertical surface displacements using GRACE and GPS over Shanxi province. *Geomat. Inf. Sci. Wuhan Univ.* **2013**, *38*, 426–430.
15. Chenchao, Z.; Liu, R. Vertical deformation of seasonal hydrological loading in southern Tibet detected by joint analysis of GPS and GRACE. *Geomat. Inf. Sci. Wuhan Univ.* **2018**, *43*, 669–675.
16. Wang, L.S.; Chen, C.; Zou, R.; Du, J.S.; Chen, X.D. Using GPS and GRACE to detect seasonal horizontal deformation caused by loading of terrestrial water: A case study in the Himalayas. *Chin. J. Geophys.* **2014**, *57*, 1792–1804. (In Chinese)
17. Godah, W.; Ray, J.D.; Szelachowska, M.; Krynski, J. The Use of National CORS Networks for Determining Temporal Mass Variations within the Earth's System and for Improving GRACE/GRACE-FO Solutions. *Remote Sens.* **2020**, *12*, 3359. [CrossRef]
18. Zhang, T.; Shen, W.B.; Pan, Y.; Luan, W. Study of seasonal and long-term vertical deformation in Nepal based on GPS and GRACE observations. *Adv. Space Res.* **2018**, *61*, 120–121. [CrossRef]
19. Ray, J.D.; Vijayan, M.; Godah, W. Seasonal horizontal deformations obtained using GPS and GRACE data: Case study of North-East India and Nepal Himalaya. *Acta Geod. Et Geophys.* **2021**, *56*, 61–76. [CrossRef]
20. Lenczuk, A.; Leszczuk, G.; Klos, A.; Kosek, W.; Bogusz, J. Study on the inter-annual hydrology-induced displacements in Europe using GRACE and hydrological models. *J. Appl. Geod.* **2020**, *14*, 393–403. [CrossRef]
21. Xiong, J.; Yin, J.; Guo, S.; Slater, L. Continuity of terrestrial water storage variability and trends across mainland China monitored by the GRACE and GRACE-Follow on satellites. *J. Hydrol.* **2021**, *599*, 126308. [CrossRef]
22. Feng, W.; Wang, C.Q.; Mu, D.P.; Zhong, M.; Zhong, Y.L.; Xu, H.Z. Groundwater storage variations in the North China Plain from GRACE with spatial constraints. *Chin. J. Geophys.* **2017**, *60*, 1630–1642.
23. Zhong, Y.; Zhong, M.; Feng, W.; Zhang, Z.; Shen, Y.; Wu, D. Groundwater Depletion in the West Liaohe River Basin, China and its implications revealed by GRACE and in situ measurements. *Remote Sens.* **2018**, *10*, 493. [CrossRef]
24. Li, J.; Chen, J.L.; Wilson, C.R. Topographic effects on coseismic gravity change for the 2011 Tohoku-Oki earthquake and comparison with GRACE. *J. Geophys. Res. Solid Earth* **2016**, *121*, 5509–5537. [CrossRef]
25. Matsuo, K.; Heki, K. Coseismic and postseismic gravity changes of the 2011 Tohoku-Oki Earthquake from satellite gravimetry. In *AGU Fall Meeting Abstracts*; ADS: Washington, DC, USA, 2011; p. G51A-0872.
26. Swenson, S.; Chambers, D.; Whar, J. Estimating geocenter variations from a combination of GRACE and ocean model output. *J. Geophys. Res.* **2008**, *113*, 1–12. [CrossRef]
27. Li, X.; Zhong, B.; Li, J.; Liu, R. Analysis of terrestrial water storage changes in the Shaan-Gan-Ning Region using GPS and GRACE/GFO. *Geod. Geodyn.* **2022**, *11*, 1–10. [CrossRef]
28. Herring, T.A.; King, R.W.; Floyd, M.A.; McClusky, S.C. Introduction to GAMIT/GLOBK. Available online: http://geoweb.mit.edu/gg/Intro_GG.pdf (accessed on 2 June 2018).
29. Farrell, W.E. Deformation of the Earth by surface loads. *Rev. Geophys.* **1972**, *10*, 761–797. [CrossRef]
30. Zhang, Z.Z.; Chao, B.F.; Lu, Y.; Hsu, H.T. An effective filtering for GRACE time-variable gravity: Fan filter. *Geophys. Res. Lett.* **2009**, *36*, L17311. [CrossRef]
31. Wang, H.; Xiang, L.; Jiang, L.; Wang, Z.; Bo, H.; Peng, G. Load Love numbers and Green's functions for elastic Earth models PREM, iasp91, ak135, and modified models with refined crustal structure from Crust 2.0. *Comput. Geosci.* **2012**, *49*, 190–199. [CrossRef]
32. Tapley, B.D.; Bettadpur, S.; Watkins, M.; Reiger, C. The gravity recovery and climate experiment: Mission overview and early results. *Geophys. Res. Lett.* **2004**, *31*, L09607. [CrossRef]
33. Chen, J.L.; Rodell, M.; Wilson, C.R.; Famiglietti, J.S. Low degree spherical harmonic influences on Gravity Recovery and Climate Experiment (GRACE) water storage estimates. *Geophys. Res. Lett.* **2005**, *32*, L14405. [CrossRef]

34. Zhong, Y.; Zhong, M.; Mao, Y.; Ji, B. Evaluation of Evapotranspiration for Exorheic Catchments of China During the GRACE Era: From a Water Balance Perspective. *Remote Sens.* **2020**, *12*, 511. [CrossRef]
35. Landerer, F. Monthly Estimates of Degree-1 (geocenter) Gravity Coefficients, Generated from GRACE (04-2002—6/2017) and GRACE-FO (06/2018 onward) RL06 Solutions, GRACE Technical Note 13, the GRACE Project, NASA Jet Propulsion Laboratory. 2019. Available online: https://podaac-tools.jpl.nasa.gov/drive/files/allData/grace/docs (accessed on 30 December 2019).
36. Loomis, B.D.; Rachlin, K.E.; Wiese, D.N.; Landerer, F.W.; Luthcke, S.B. Replacing GRACE/GRACE-FO C30 with satellite laser ranging: Impacts on Antarctic Ice Sheet mass change. *Geophys. Res. Lett.* **2020**, *47*, e2019GL085488. [CrossRef]
37. Save, H.; Tapley, B.; Bettadpur, S.; CSR Level-2 Team. "GRACE RL06 Reprocessing and Results from CSR" EGU2018-10697. *EGU Gen. Assem.* **2018**. Available online: https://ui.adsabs.harvard.edu/abs/2018EGUGA..2010697S/abstract (accessed on 30 April 2018).
38. Liu, R.; Li, J.; Fok, H.S.; Shum, C.K.; Li, Z. Earth surface deformation in the north China plain detected by joint analysis of GRACE and GPS data. *Sensors* **2014**, *14*, 19861–19876. [CrossRef]
39. Li, W.; Dong, J.; Wang, W.; Wen, H.; Liu, H.; Guo, Q.; Yao, G.; Zhang, C. Regional Crustal Vertical Deformation Driven by Terrestrial Water Load Depending on CORS Network and Environmental Loading Data: A Case Study of Southeast Zhejiang. *Sensors* **2021**, *21*, 7699. [CrossRef]
40. Jiang, W.; Wang, K.; Deng, L.; Li, Z. Impact on nonlinear vertical variation of GNSS vertical variation of GNSS reference stations caused by thermal expansion. *Acta Geod. Et Cartogr. Sin.* **2015**, *44*, 473–480.
41. Guo, J.; Mu, D.; Liu, X.; Yan, H.; Sun, Z.; Guo, B. Water storage changes over the Tibetan Plateau revealed by GRACE mission. *Acta Geophys.* **2016**, *64*, 463–476. [CrossRef]
42. Guo, J.; Mu, D.; Liu, X.; Yan, H.; Dai, H. Equivalent water height extracted from GRACE gravity field model with robust independent component analysis. *Acta Geophys.* **2014**, *62*, 953–972. [CrossRef]
43. Yao, G.; Yilmaz, A.; Zhang, L.; Meng, F.; Ai, H.; Jin, F. Matching large baseline oblique stereo images using an end-to-end convolutional neural network. *Remote Sens.* **2021**, *13*, 274. [CrossRef]